Inhibition of Lipid A Biosynthesis as the Primary Mechanism of CHIR-090 Antibiotic Activity in *Escherichia coli*†

Adam W. Barb, Amanda L. McClerren, Karnem Snehelatha, C. Michael Reynolds, Pei Zhou, and Christian R. H. Raetz*

Department of Biochemistry, Duke University Medical Center, Durham, North Carolina 27710

Received December 6, 2006; Revised Manuscript Received January 24, 2007

ABSTRACT: The deacetylation of UDP-3-*O*-[(*R*)-3-hydroxymyristoyl]-*N*-acetylglucosamine (UDP-3-*O*-acyl-GlcNAc) by LpxC is the committed reaction of lipid A biosynthesis. CHIR-090, a novel *N*-aroyl-L-threonine hydroxamic acid, is a potent, slow, tight-binding inhibitor of the LpxC deacetylase from the hyperthermophile *Aquifex aeolicus*, and it has excellent antibiotic activity against *Pseudomonas aeruginosa* and *Escherichia coli*, as judged by disk diffusion assays. We now report that CHIR-090 is also a two-step slow, tight-binding inhibitor of *E. coli* LpxC with $K_i = 4.0$ nM, $K_i^* = 0.5$ nM, $k_5 = 1.9$ min^{-1}, and $k_6 = 0.18$ min^{-1}. CHIR-090 at low nanomolar levels inhibits LpxC orthologues from diverse Gram-negative pathogens, including *P. aeruginosa*, *Neisseria meningitidis*, and *Helicobacter pylori*. In contrast, CHIR-090 is a relatively weak competitive and conventional inhibitor (lacking slow, tight-binding kinetics) of LpxC from *Rhizobium leguminosarum* ($K_i = 340$ nM), a Gram-negative plant endosymbiont that is resistant to this compound. The K_M (4.8 μM) and the k_{cat} (1.7 s^{-1}) of *R. leguminosarum* LpxC with UDP-3-*O*-[(*R*)-3-hydroxymyristoyl]-*N*-acetylglucosamine as the substrate are similar to values reported for *E. coli* LpxC. *R. leguminosarum* LpxC therefore provides a useful control for validating LpxC as the primary target of CHIR-090 in vivo. An *E. coli* construct in which the chromosomal *lpxC* gene is replaced by *R. leguminosarum lpxC* is resistant to CHIR-090 up to 100 μg/mL, or 400 times above the minimal inhibitory concentration for wild-type *E. coli*. Given its relatively broad spectrum and potency against diverse Gram-negative pathogens, CHIR-090 is an excellent lead for the further development of new antibiotics targeting the lipid A pathway.

The emergence of multidrug-resistant bacteria in hospital and community clinics has created an urgent need for new antibiotics (*1*, *2*). About half of the multidrug-resistant bacteria are Gram-negative pathogens (*2*), including strains of *Escherichia coli*, *Pseudomonas aeruginosa* (*1*), and *Acinetobacter baumannii* (*3*). Inhibitors that exploit traditional antibiotic targets, such as peptidoglycan, DNA replication, or protein biosynthesis (*4*), are becoming less effective (*2*). These obstacles could be overcome by developing inhibitors of novel targets required for bacterial growth (*5*, *6*).

The biosynthesis of the lipid A component of lipopolysaccharide (LPS),[1] a unique, outer-membrane lipid that shields Gram-negative bacteria from environmental stresses (*7*, *8*), is a promising target for new antibiotic development (*9*−*12*). The lipid A moiety of LPS is a hexaacylated disaccharide of glucosamine (*7*, *8*) (Figure 1). Although inhibition of any one of the first six enzymes of lipid A biosynthesis is lethal to *E. coli* (*8*), the most promising target identified to date is LpxC (*9*−*12*), a unique deacetylase that is selective for UDP-3-*O*-[(*R*)-3-hydroxymyristoyl]-*N*-acetylglucosamine (UDP-3-*O*-acyl-GlcNAc) (*13*−*16*) (Figure 1). Although LpxC catalyzes the second reaction of the lipid A pathway, it represents the committed step (Figure 1).

LpxC is a zinc-dependent amidase with a catalytic mechanism related to that of carboxypeptidase and thermolysin (*17*−*19*). *Aquifex aeolicus* LpxC, the structure of which was recently solved by both NMR spectroscopy (*18*, *20*) and X-ray crystallography (*21*, *22*), displays a novel "β-α-α-β sandwich" fold (Figure 2A). A unique feature of LpxC is a hydrophobic passage, leading away from the active site zinc ion, which accommodates the acyl chain of the substrate-mimetic inhibitor TU-514 (Figure 2A) and is presumed to capture the acyl chain of the substrate (*18*, *20*, *22*). The terminal methyl group of the TU-514 acyl chain protrudes through an opening at the surface of the enzyme (*18*, *20*).

Most of the available LpxC inhibitors that display significant antibiotic activity resemble TU-514 in that they contain a hydroxamic acid moiety to coordinate the catalytic zinc ion (*9*−*12*, *23*, *24*) (Figure 2B). However, many LpxC inhibitors, such as L-161,240 and BB-78485 (Figure 2B), which kill *E. coli*, have little or no effect on *P. aeruginosa*

† This research was supported by NIH Grants GM-51310 to C.R.H.R. and AI-055588 to P.Z. A.W.B. was supported by Cellular and Molecular Biology Training Grant GM-07184 to Duke University.

* Author to whom correspondence should be addressed. Phone: (919) 684-5326. Fax: (919) 684-8885. E-mail: raetz@biochem.duke.edu.

[1] Abbreviations: ACP, acyl carrier protein; DMSO, dimethyl sulfoxide; DTT, dithiothreitol; Kdo, 3-deoxy-D-*manno*-octulosonic acid; IC_{50}, concentration of half-maximal inhibition; IPTG, isopropyl β-D-thiogalactopyranoside; LPS, lipopolysaccharide; MIC, minimal inhibitory concentration; NMR, nuclear magnetic resonance; ORF, open reading frame; PCR, polymerase chain reaction; SDS−PAGE, sodium dodecyl sulfate−polyacrylamide gel electrophoresis; UDP-3-*O*-acyl-GlcNAc, UDP-3-*O*-[(*R*)-3-hydroxymyristoyl]-*N*-acetylglucosamine; UDP-GlcNAc, UDP-*N*-acetylglucosamine.

10.1021/bi6025165 CCC: $37.00
Published on Web 03/03/2007

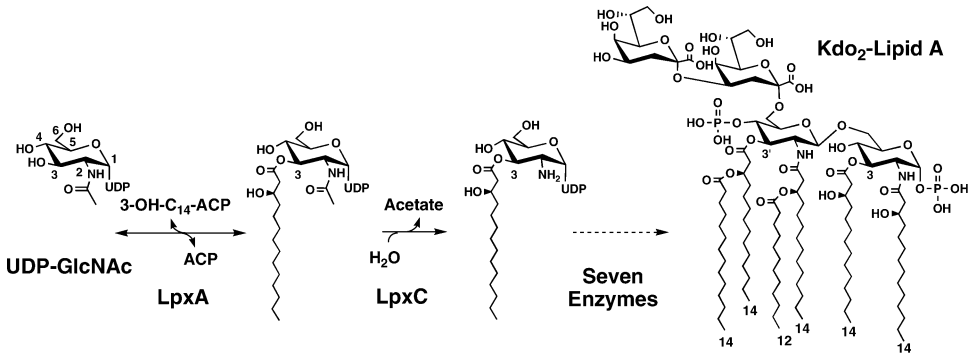

FIGURE 1: Reaction catalyzed by LpxC and structure of *E. coli* lipid A. The biosynthesis of lipid A begins with the 3-O-acylation of UDP-GlcNAc by the cytosolic enzyme LpxA (*8*). In the first irreversible (committed) reaction of the pathway, the deacetylase LpxC unblocks the nitrogen at the 2 position of the glucosamine ring (*8*). Seven downstream enzymes produce Kdo_2-lipid A (*8*), the hydrophobic membrane anchor of LPS, and a potent toll-like receptor 4 agonist (*44*).

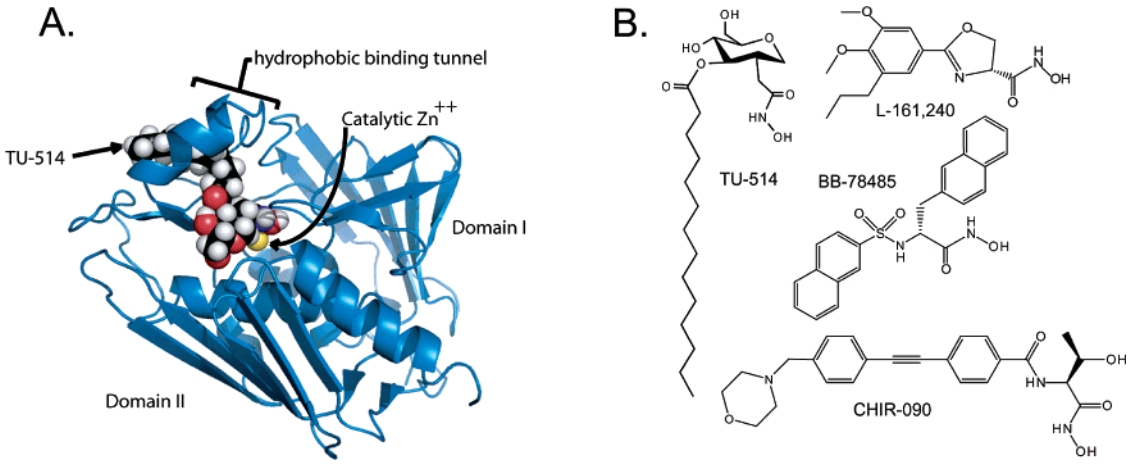

FIGURE 2: Structures of *A. aeolicus* LpxC and of various LpxC inhibitors. Panel A: The three-dimensional structure of LpxC is characterized by a unique "β-α-α-β sandwich" fold (*18*, *20*−*22*). The NMR structure of LpxC was solved with one bound molecule of the substrate analogue TU-514 (*18*, *20*). LpxC contains an unusual hydrophobic tunnel that encapsulates the acyl chain of TU-514 (*18*, *20*, *22*). This figure was generated with PyMol using the Protein Data Bank accession code 1XXE. Panel B: All relevant LpxC inhibitors contain a zinc-chelating hydroxamate moiety. Structures of LpxC complexes including other inhibitors are not yet available.

(*10*, *12*). This anomaly is explained by the fact that *P. aeurginosa* LpxC is only 55% identical to *E. coli* LpxC, and its activity is much less susceptible to inhibition by L-161,-240 and BB-78485 (*25*).

McClerren et al. recently reported CHIR-090 (Figure 2B), a very potent, slow, tight-binding inhibitor of *A. aeolicus* LpxC (*11*), the sequence of which is 31% identical to *E. coli* LpxC. McClerren et al. also showed that CHIR-090 has remarkable antibiotic activity against *E. coli* and *P. aeruginosa*, comparable to ciprofloxacin, as judged by disk diffusion assays (*11*). However, the inhibition of LpxC from these and other pathogenic bacteria by CHIR-090 was not fully evaluated. It also remains unclear whether or not LpxC is the sole target of CHIR-090 in vivo. We now report that CHIR-090 is a slow, tight-binding inhibitor of *E. coli* LpxC with $K_i = 4.0$ nM, $K_i^* = 0.5$ nM, $k_5 = 1.9$ min^{-1}, and $k_6 = 0.18$ min^{-1}. CHIR-090 inhibits LpxC orthologues from several other important Gram-negative pathogens at low nanomolar concentrations. In contrast, however, both growth and LpxC activity of the Gram-negative plant endosymbiont *Rhizobium leguminosarum* are insensitive to CHIR-090. Replacement of *E. coli lpxC* by *R. leguminosarum lpxC* renders *E. coli* fully resistant at 400 times the minimal inhibitory concentration (MIC) for wild-type cells, demonstrating that LpxC is the primary target for CHIR-090 in vivo.

EXPERIMENTAL PROCEDURES

Materials, Strains, and Reagents. PEI-cellulose TLC plates were purchased from EMD Chemicals, Gibbstown, NJ. Bovine serum albumin (BSA), imidazole, HEPES, and sodium phosphate were obtained from Sigma-Aldrich, St. Louis, MO, and [α-^{32}P]UTP was purchased from NEN DuPont. Ni-NTA agarose resin and plasmid miniprep kits were purchased from Qiagen, Valencia, CA. Coomassie-Plus protein reagent and GelCode blue staining reagent were purchased from Pierce, Rockford, IL. *E. coli* BLR(DE3)/pLysS, *E. coli* XL1-Blue competent cells, and *Pfu* polymerase were purchased from Stratagene, La Jolla, CA. The vector pET21b was purchased from Novagen (an EMD Chemicals Co.). Primers were purchased from MWG Biotech, High Point, NC. Restriction endonucleases *Nde*I and *Bam*HI were purchased from New England Biolabs, Ipswich, MA. Genomic DNA from *R. leguminosarum* strain 3841 was prepared as described previously (*26*), and DNA from *Helicobacter pylori* was provided by Dr. M. Stephen Trent, East Tennessee State University, Johnson City, TN. Genomic DNA from *Neisseria meningiditis* (ATCC 700532D) was purchased from the American Type Culture Collection, Manassas, VA. *P. aeruginosa lpxC* cloned into pET21b was constructed as previously described (*27*). The LpxC inhibitor CHIR-090 was prepared at the Duke University Small

Molecule Synthesis Facility according to published procedures (*28*).

Cloning of lpxC Genes from H. pylori, N. meningiditis, and R. leguminosarum. The *lpxC* genes from *H. pylori*, *N. meningitidis*, and *R. leguminosarum* were amplified from genomic DNA by PCR, using the primers listed in Table S1, and cloned into a pET21b vector in-frame with the C-terminal His tag. The presence of the correct insert was confirmed by DNA sequencing.

Overexpression and Purification of H. pylori, N. meningiditis, and R. leguminosarum LpxC. The purification and specific activity of each LpxC orthologue is summarized in Table S2. Plasmids containing C-terminal His-tagged *lpxC* genes from *H. pylori*, *N. meningiditis*, and *R. leguminosarum* were transformed into *E. coli* BLR (DE3)/pLysS competent cells for overexpression. Overnight cultures (5 mL) were grown from single colonies at 37 °C in LB broth (*29*), containing 100 μg/mL ampicillin and 25 μg/mL chloramphenicol, and used to inoculate 50 mL of LB broth, supplemented with the same antibiotics. These cultures were grown to an A_{600} of 0.5. LpxC expression was induced with 1 mM isopropyl β-D-thiogalactopyranoside (IPTG) in the presence of 100 μM $ZnSO_4$. All cultures were grown at 25 °C for an additional 5 h and then harvested at 6000*g* for 20 min at 4 °C. The cell pellets were resuspended in 25 mL of 25 mM HEPES, pH 7.0, containing 2 mM β-mercaptoethanol, 300 mM NaCl, and 20% glycerol. The cells were broken by three passages through a cold French pressure cell at 18000 psi, and debris was removed by centrifugation at 8000*g* for 20 min at 4 °C. The supernatant was loaded onto a 5 mL Ni-NTA agarose column and equilibrated with 5 mM HEPES, pH 7.0, containing 2 mM β-mercaptoethanol, 300 mM NaCl, and 20% glycerol, and the protein was eluted with 200 mM imidazole. The fractions containing LpxC were pooled, concentrated, and dialyzed into 25 mM HEPES, pH 7.0, containing 2 mM DTT, 150 mM NaCl, and 10% glycerol. Protein concentrations were determined using the bicinchoninic assay (*30*).

Overexpression and Purification of E. coli LpxC and P. aeruginosa LpxC Lacking His Tags. *E. coli* LpxC was prepared as previously described (*18*) using *lpxC* expressed in pET11a (*31*). For *P. aeruginosa* LpxC, a fresh colony of BLR(DE3)/pLysS harboring *P. aeruginosa lpxC* cloned into pET21b was used to inoculate 5 mL of LB broth for an overnight culture. *P. aeruginosa* LpxC was cloned without the His tag present on pET21b. A 1.5 L portion of M9 medium (*29*), containing 100 μg/mL ampicillin and 25 μg/mL chloramphenicol, was inoculated with the overnight culture. Cells were grown at 37 °C to an A_{600} of 0.5, and then IPTG was added to 1 mM. The bacterial cells were subsequently grown at 30 °C for 3 h, harvested, and lysed as described above. Next, 13.5 g of ammonium sulfate was added to 43 mL of cytosol, and the mixture was incubated on ice for 1.5 h. Protein precipitate was recovered by centrifugation at 8000*g* for 20 min, and it was resuspended in 30 mL of 25 mM HEPES, pH 7.0, containing 10% glycerol and 2 mM DTT. Remaining ammonium sulfate was removed by overnight dialysis against the same buffer.

The sample was applied to a 30 mL Q-Sepharose (Amersham-Pharmacia) column equilibrated with the same buffer. The column was eluted with a linear gradient of 0−1 M KCl dissolved in 25 mM HEPES, pH 7.0, and 2 mM DTT.

Scheme 1: Two-Step Mechanism for Slow, Tight-Binding Inhibition

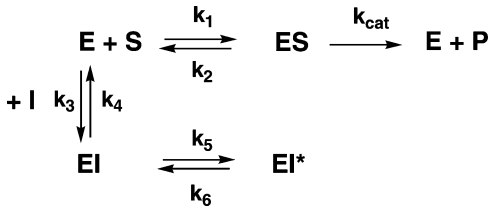

Fractions (5 mL) containing LpxC activity were pooled and concentrated to 1 mL. The protein was further purified using a 2 cm × 46 cm Sephadex G75 column (Amersham-Pharmacia) equilibrated in the same buffer. Fractions (2 mL) containing LpxC activity were pooled, and purity was assessed by SDS−PAGE. The protein was stored at −80 °C prior to being assayed. Electrospray ionization mass spectrometry (*11*) was used to confirm the exact mass predicted from the *P. aeruginosa* LpxC sequence. SDS−PAGE analysis of each of the above LpxC preparations showed no more than 10% contaminating proteins, as judged by densitometry.

Assay of LpxC Activity. UDP-3-*O*-[(*R*)-3-hydroxymyristoyl]-*N*-acetylglucosamine and [α-^{32}P]UDP-3-*O*-[(*R*)-3-hydroxymyristoyl]-*N*-acetylglucosamine were prepared enzymatically as previously described (*31*). Assays of LpxC activity were performed with 5 μM substrate, except where noted (*11*); additionally, 10% DMSO was added to the assay mixtures and held constant at that level when inhibitor (dissolved in DMSO) was added. Except where noted, the concentration of the enzyme was at least 10-fold less than the concentration of either the inhibitor or the substrate. When preincubated with or without inhibitor prior to being assayed, the enzyme was diluted in 25 mM sodium phosphate, pH 7.4, containing 1 mg/mL BSA and 10% DMSO. The preincubation mixture was held on ice for 15 min before the reaction was initiated by means of a 1:4 dilution of the enzyme into the assay cocktail. Initial velocities were calculated from the linear portion of reaction progress curves (<10% conversion of substrate to product).

Determination of the Mechanism of CHIR-090 Binding to E. coli LpxC. In order to assess the slow, tight-binding phenomenon, 0.2 nM *E. coli* LpxC was first assayed in the presence of 0, 0.5, 1, 2, 3, 4, 6, or 8 nM inhibitor without any preincubation. In these assays, 2.2×10^6 dpm of [α-^{32}P]-UDP-3-*O*-[(*R*)-3-hydroxymyristoyl]-*N*-acetylglucosamine was included per reaction. Equation 1, describing time-dependent inhibition, was fitted to the data as previously described (Scheme 1) (*11*). The rate of EI* formation (k_{obs}) was determined from curve fitting with

$$[P] = v_s t + [(v_i - v_s)/k_{obs}][1 - \exp(-k_{obs} t)] + C \quad (1)$$

where [P] is the concentration of product at time t, v_i is the initial velocity, v_s is the steady-state velocity, and k_{obs} is the first-order exponential term for the formation of the EI* complex.

A modified form of eq 1 was used to fit the rate of formation of free E (k'_{obs}) by measuring product accumulation after a 100-fold rapid dilution following a 60 min preincubation (*32*). The time-dependent inhibition equation was modified by setting the initial velocity (v_i) to 0 and was

subsequently rearranged:

$$[P] = v_s t - (v_s/k'_{obs})[1 - \exp(-k'_{obs} t)] + C \quad (2)$$

The microscopic rate constants defining the rate of the formation and dissociation of the EI* complex in Scheme 1 were computed from

$$k_{obs} = k_6 + k_5/[1 + (IC_{50}/[I])] \quad (3)$$

where k_5 and k_6 are defined as described by Morrison (*11*, *32*, *33*), IC_{50} was determined by fitting the IC_{50} equation to the initial velocities, and [I] is the concentration of CHIR-090 in the assay. The K_i* describing the potency of CHIR-090 after the onset of time-dependent inhibition was derived using

$$K_i^* = K_i/[1 + (k_5/k_6)] \quad (4)$$

K_i* for *E. coli* LpxC was determined by independently varying CHIR-090 from 50 pM to 4 nM, keeping the concentration of enzyme constant at 0.2 nM. The Morrison equation was then fitted to the data (*32*):

$$v_i/v_o = 1 - [([E]_T + [I]_T + K_i^*) - \sqrt{([E]_T + [I]_T + K_i^*)^2 - 4[E]_T[I]_T}]/2[E]_T \quad (5)$$

where v_i is the initial velocity of the reaction, v_o is the velocity of the uninhibited reaction, $[E]_T$ is the empirically determined total enzyme concentration, and $[I]_T$ is the total concentration of CHIR-090.

Determination of Kinetic Parameters for E. coli and R. leguminosarum LpxC. K_M and V_{max} were determined by varying the substrate from 0.5 to 50 μM for *E. coli* LpxC and from 1 to 100 μM for *R. leguminosarum* LpxC. Data were analyzed using an Eadie−Hofstee plot (*34*) and by a nonlinear curve-fitting program (KaleidaGraph; Synergy Software); the resultant values were nearly identical and within the error of the experiment. To determine a K_i for CHIR-090 against *R. leguminosarum* LpxC, CHIR-090 concentrations were varied from 0.1 to 50 μM, and an equation describing a binding isotherm was fit to the data (*32*). A K_i value was calculated using

$$K_i = IC_{50}/[1 + ([S]/K_M)] \quad (6)$$

Construction of E. coli W3110RL. In this strain, *R. leguminosarum lpxC* was used to replace *E. coli lpxC*. A PCR product containing the *R. leguminosarum* ORF was amplified from *R. leguminosarum* genomic DNA. PCR was used to construct a linear piece of DNA containing *R. leguminosarum lpxC* (primers shown in Table S1), flanked on the 5′ end by 40 bp of DNA complementary to the 5′ region upstream of *E. coli lpxC* and on the 3′ end by 40 bp of DNA complementary to the 3′ region downstream of *E. coli lpxC*. This fragment was extracted from an agarose gel, purified using a Qiagen PCR cleanup kit, and eluted with distilled water. The fragment was then electroporated into *E. coli* W3110 cells, containing the temperature-sensitive pDK46 recombination plasmid (*35*), using a Bio-Rad Gene Pulser II set to 2.5 kV, 25 μF, and 400 Ω. Because no CHIR-090-resistant *E. coli* W3110 colonies were observed on LB plates supplemented with 1 μg/mL CHIR-090 (data not shown), transformants could be selected directly using CHIR-090 without introducing a closely linked resistance cassette for a different antibiotic marker. Recombinant colonies containing *R. leguminosarum lpxC* were selected on LB agar plates, containing 1 μg/mL CHIR-090. Genomic DNA from resistant colonies was isolated, and the region around *lpxC* was sequenced. One clone in which *R. leguminosarum lpxC* had replaced *E. coli lpxC* was selected and grown at 37 °C to eliminate the pKD46 plasmid. This strain was subsequently named *E. coli* W3110RL.

$P1_{vir}$ Transduction Experiments. E. coli W3110RL was transduced to kanamycin resistance using a $P1_{vir}$ lysate prepared on *E. coli* Δ*yacF-21* (strain EDCM371 obtained from the *E. coli* Genetic Resource Center at Yale University, which contains a kanamycin resistance cassette near LpxC around minute 2 on the *E. coli* chromosome). More than 100 kanamycin-resistant colonies were recovered, and 12 were restreaked onto fresh LB plates containing kanamycin (25 μg/mL); these were then tested on LB plates containing 1 μg/mL CHIR-090 to verify the genetic linkage of kanamycin and CHIR-090 resistance in W3110RL.

LpxC Activity in Cell-Free Lysates. E. coli W3110 and W3110RL were each grown to an A_{600} of 0.6 and harvested at 4000*g* for 15 min at 4 °C. Cell pellets were resuspended in 2 mL of 25 mM HEPES, pH 7.0, containing 2 mM DTT, and lysed by three passages through a cold French pressure cell at 18000 psi. Lysates were cleared by centrifugation at 8000*g* for 20 min at 4 °C. LpxC activity was determined as described above, except that 0.5 mM AMP was included to inhibit CDP-diglyceride hydrolase-catalyzed cleavage of the substrate (*16*).

Disk Diffusion Assays of Antibiotic Sensitivity and Bacterial Growth Tests. Disk diffusion was conducted as previously described (*11*), except that 10 μg of each antibiotic compound was used per filter. Growth in liquid medium in the presence of CHIR-090 was evaluated as follows: Cells from overnight cultures were inoculated into 50 mL portions of LB broth at an A_{600} of 0.02 and grown with shaking at 30 °C. When the A_{600} reached 0.15, parallel cultures were treated with either 6 μL of 500 μg/mL CHIR-090 in DMSO or 6 μL of DMSO. To assess cumulative growth, cultures were maintained in log phase growth by 10-fold dilution into prewarmed medium, containing the same concentrations of DMSO or DMSO/CHIR-090, whenever the A_{600} reached 0.4.

Antibiotic Minimal Inhibitory Concentrations. The minimal inhibitory concentration was defined as the lowest antibiotic concentration at which no measurable bacterial growth was observed in LB medium containing 1% DMSO (v/v), when inoculated at a starting density of $A_{600} = 0.01$. Cultures were incubated with shaking for 24 h at 30 °C in the presence of CHIR-090. Experiments were performed in triplicate.

RESULTS

CHIR-090 Is a Two-Step, Slow, Tight-Binding Inhibitor of E. coli LpxC. CHIR-090 is a competitive, two-step, slow, tight-binding inhibitor of *A. aeolicus* LpxC (Scheme 1) (*11*). Although CHIR-090 also inhibits *E. coli* LpxC in the low nanomolar range and has potent antibiotic activity against this organism (*11*), the mechanism of inhibition of the *E. coli* enzyme was not previously determined. We therefore investigated the question of whether or not CHIR-090 is a

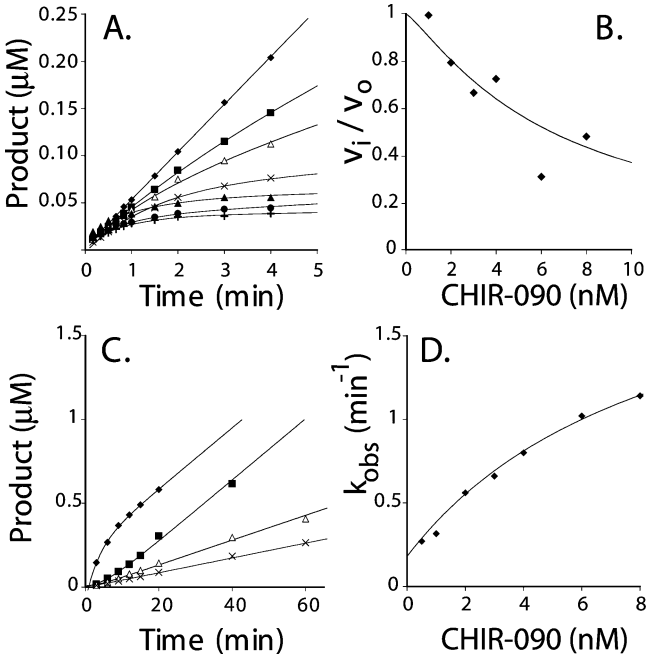

FIGURE 3: Slow, tight-binding inhibition of *E. coli* LpxC by CHIR-090. Panel A: Progress curves for product formation when reactions are started by addition of enzyme in the presence of 0 nM (◆), 1 nM (■), 2 nM (△), 3 nM (×), 4 nM (▲), 6 nM (●), or 8 nM (+) CHIR-090. Panel B: Plot of fractional velocities extracted from the results in panel A as a function of CHIR-090 concentration. A standard IC_{50} equation was fit to the data with an IC_{50} of 9 nM. Panel C: Progress curves obtained after rapid dilution of *E. coli* LpxC preincubated with CHIR-090. Key: (◆) control reaction in which 0.25 nM LpxC was used to start the reaction in the presence of 0.5 nM CHIR-090; (■) preincubation of 50 nM CHIR-090 with 25 nM LpxC diluted 100 times into the assay mixture; (△) preincubation of 100 nM CHIR-090 with 25 nM LpxC diluted 100 times into the assay mixture; (×) preincubation of 200 nM CHIR-090 with 25 nM LpxC diluted 100 times into the assay mixture. Preincubations were done at 30 °C . Panel D: A plot of the observed first-order rate constant for the formation of the EI* complex as fitted with eq 3. The *Y*-intercept (0.18 min^{-1}) was determined independently from the dilution experiment shown in panel C. A repeat experiment (not shown) gave identical results (within 10%).

time-dependent inhibitor of *E. coli* LpxC. Equation 1 was fitted to the data from reaction progress curves (Figure 3A), which clearly show slow, tight-binding behavior. Analysis of the data from the first minute of the reaction (Figure 3B) demonstrates that CHIR-090 reduces the initial rate of deacetylation, consistent with a two-step mechanism (Scheme 1).

The first-order rate constant describing the formation of the EI* complex (k_{obs}) was plotted as a function of inhibitor concentration (Figure 3D). The hyperbolic nature of this plot is likewise indicative of a two-step mechanism (Scheme 1) (*11*, *33*). An additional numeric constraint for k_6, which describes the reversal of the EI* complex to the EI complex (Scheme 1), was determined independently using a rapid dilution method (*32*). *E. coli* LpxC (25 nM) was preincubated with 50, 100, or 200 nM CHIR-090 and then diluted 100-fold into a reaction mixture containing 5 μM substrate. The progress curves show that enzyme activity slowly returns (Figure 3C), consistent with the formation of free enzyme. Equation 2 was fit to the data shown in Figure 3C, and a value for k'_{obs}, representative of the microscopic rate constant k_6, of 0.18 min^{-1} was determined. This value was similar to the value determined when the CHIR-090 concentration was extrapolated to zero in Figure 3D. The k'_{obs} for this transition provides a lower bound for the true k_6.

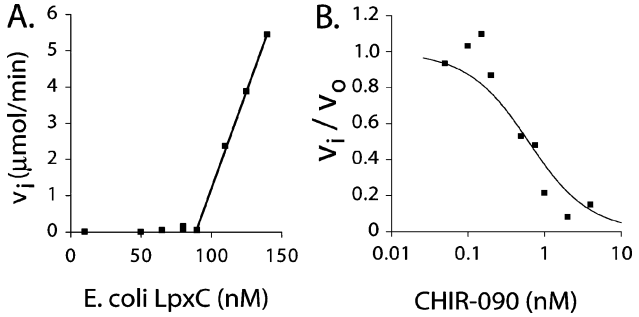

FIGURE 4: Determination of K_i* under conditions of similar enzyme and CHIR-090 concentration. A plot of initial velocity measurements with different amounts of *E. coli* LpxC in the presence of 100 nM CHIR-090 is shown in panel A. The active enzyme concentration was determined by extrapolating to zero a line representing the linear fit of reactions with measurable activity. For these data, this line intersects the *x*-axis at 90 nM, suggesting the active enzyme concentration is within 10% of the enzyme concentration estimated by UV absorption. In panel B, fractional activity (v_i/v_o) was measured over a range of CHIR-090 concentrations, where the amount of enzyme was held constant at 0.2 nM. Using the active enzyme concentration calculated from the data shown in panel A, eq 5 was fitted to the data in panel B, yielding a K_i* value of 0.5 ± 0.1 nM. A repeat experiment (not shown) gave identical results (within 10%).

Using the estimated value of k_6, eq 3 was fit to the data shown in Figure 3D, yielding a value of 1.9 ± 0.3 min^{-1} for k_5 (*32*, *33*). Further analysis, using eqs 3 and 4, yielded a K_i of 4.0 ± 1.0 nM (describing k_4/k_3) (*33*) and an overall inhibition constant (K_i*) of 0.4 ± 0.1 nM. Analysis of the microscopic rate constants predicts a half-life of 20 s for the formation of the EI* complex, not dissimilar to the value of 56 s determined for *A. aeolicus* LpxC (*11*). In the latter case, however, EI* formation is irreversible.

To confirm the K_i* determined from the microscopic rate constants, we measured the residual activity of *E. coli* LpxC after the slow-binding step had reached equilibrium. In order to use the Morrison equation (eq 5) to derive K_i*, it was necessary to know the *active* enzyme concentration. This value was determined by finding the concentration at which LpxC activity became measurable when the protein was titrated into a reaction mixture containing 100 nM CHIR-090 (*32*). By this criterion the active enzyme concentration was within 10% of the estimated total protein concentration, as determined by A_{280} as previously described (Figure 4A) (*31*). *E. coli* LpxC (0.2 nM) was next assayed in the presence of 0.05−4 nM inhibitor (Figure 4B). In this case, the reaction rates were determined from the linear portions of the progress curves after the full onset of slow, tight-binding inhibition (or 5 min into the reaction). The K_i* value determined using eq 5 (0.5 ± 0.1 nM) was similar to that determined by the curve fitting method described above (0.4 ± 0.1 nM).

CHIR-090 Is a Potent Inhibitor of Diverse LpxC Orthologues. We next determined whether or not CHIR-090 inhibits LpxCs from other Gram-negative organisms. Four diverse LpxC orthologues (*P. aeruginosa*, *H. pylori*, *N. meningiditis*, and *R. leguminosarum*), which share 57%, 43%, 49%, and 43% sequence identity to *E. coli* LpxC, respectively, were chosen. To measure the potency of CHIR-090 inhibition against these orthologues, we compared the initial reaction velocities under standard assay conditions using

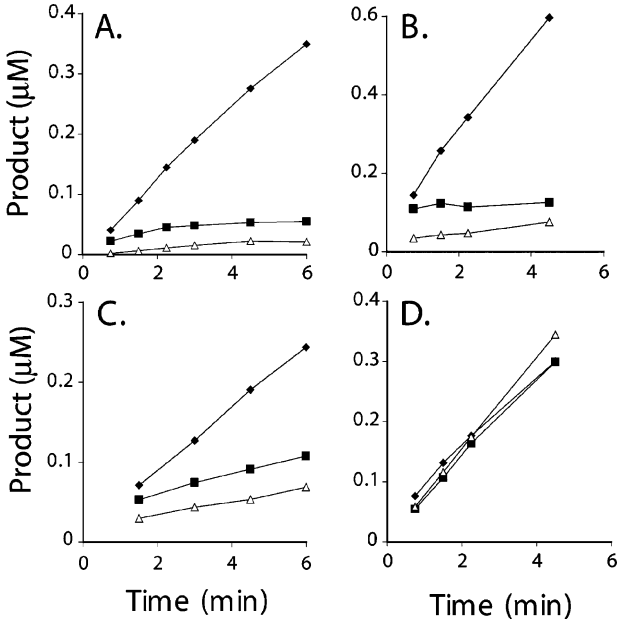

FIGURE 5: Effect of CHIR-090 on diverse LpxC orthologues. In each panel the symbols indicate the following order of addition: (◆) the CHIR-090 concentration was 16 nM during a 15 min preincubation with enzyme and 4 nM following dilution into the assay system; (■) the CHIR-090 concentration was 0 nM during the preincubation but 4 nM in the assay mixture; (△) the CHIR-090 concentration was 0 nM during the preincubation and 0 nM in the assay mixture. Panel A: *E. coli* LpxC. Panel B: *H. pylori* LpxC. Panel C: *P. aeruginosa* LpxC. Panel D: *R. leguminosarum* LpxC. *R. leguminosarum* LpxC was assayed with 10-fold higher CHIR-090 concentrations (160 nM during the preincubation and 40 nM in the assay mixture). Preincubations were done at 4 °C and reactions at 30 °C. The points are connected for ease of viewing. A repeat experiment (not shown) gave identical results (within 10%).

purified enzymes in the presence or absence of CHIR-090. As with *E. coli* LpxC (Figure 5A), *H. pylori* LpxC (Figure 5B), *P. aeruginosa* LpxC (Figure 5C), and *N. meningitidis* LpxC (data not shown) were inhibited 75% or more by 4 nM CHIR-090 when enzyme was used to start the reactions. The specific activity of the *N. meningitidis* protein was at least 20-fold less than that of the others, suggesting that the expression or assay conditions for *N. meningitidis* LpxC may not be optimal (Table S1). To investigate possible time-dependent inhibition by CHIR-090, we preincubated each enzyme with 16 nM CHIR-090 for 15 min before diluting 4-fold into the assay mixture containing the substrate. We then compared the rates and extents of product formation to those obtained without preincubation (Figure 5A−C). For the assays done without preincubation, there was considerably more product accumulation by the first time point, consistent with slow-binding inhibition in each case (Figure 5A−C). A residual slow rate of product formation was observed with each of these enzymes (Figure 5A−C), suggesting that EI* formation is reversible, in contrast to *A. aeolicus* LpxC (*11*).

CHIR-090 Is a Weak Competitive Inhibitor of R. leguminosarum LpxC. Surprisingly, *R. leguminosarum* LpxC was not inhibited by 40 nM CHIR-090 (Figure 5D) under the same conditions that showed >75% inhibition of the other orthologues by only 4 nM CHIR-090 (Figure 5A−C). There was no evidence for time-dependent inhibition with the *R. leguminosarum* enzyme (Figure 5D) at any concentration tested. Furthermore, CHIR-090 did not inhibit the growth of *R. leguminosarum*, *Rhizobium etli*, *Sinorhizobium meliloti*, or *Agrobacterium tumefaciens*, as judged by standard disk diffusion assays (data not shown) (*11*). These CHIR-090-resistant bacteria all belong to the Rhizobiaceae family, a group of soil-borne Gram-negative organisms that infect plants (*36*).

The K_M and k_{cat} of *R. leguminosarum* LpxC were determined (Table 1) as described in Experimental Procedures. The *R. leguminosarum* values were similar to those for *E. coli* and were consistent with previous studies (*31*). There was no evidence for allosteric effects or product inhibition (data not shown).

To determine the K_i of CHIR-090, the *R. leguminosarum* enzyme was assayed with 5 μM substrate in the presence of 4 nM to 50 μM inhibitor (Figure 6). Using the kinetic parameters established above and the measured IC_{50} in conjunction with eq 6 for a simple competitive inhibitor, the K_i for CHIR-090 was calculated to be 340 ± 60 nM (Table 1). There was no evidence for slow, tight-binding inhibition.

CHIR-090 Primarily Targets E. coli LpxC in Vivo. CHIR-090 is a potent antibiotic against *E. coli* and inhibits *E. coli* LpxC activity in vitro in the low nanomolar range (Figure 3). *E. coli* W3110 colonies resistant to 1 μg/mL CHIR-090 are not observed without prior chemical mutagenesis (data not shown). To determine whether or not CHIR-090 targets other enzymes besides LpxC, we constructed a strain of *E. coli* W3110 (Figure 7), designated W3110RL, in which *R. leguminosarum lpxC* replaces the chromosomal copy of *E. coli lpxC*. This strain is able to grow on LB agar plates containing 1−10 μg/mL CHIR-090, which is 4−40 times above the MIC of 0.25 μg/mL under our conditions for wild-type *E. coli* W3110 (data not shown). The doubling time of W3110RL was 40 min in the presence of 1 μg/mL CHIR-090, which is exactly the same rate as wild-type in the absence of inhibitor (Figure 8A). Wild-type cells stopped growing after about 2 h in the presence of 1 μg/mL CHIR-090 (Figure 8A).

We next tested whether or not the CHIR-090 resistance of *E. coli* W3110RL is due to the presence of *R. leguminosarum lpxC* (located at minute 2.3 on the *E. coli* chromosome) or is caused by a spontaneous mutation not linked to this locus. Transduction of *E. coli* W3110RL with a $P1_{vir}$ lysate prepared on *E. coli* Δ*yacF-21*, a strain containing a kanamycin-resistance marker at minute 2.4, generated kanamycin-resistant colonies with the expected frequency. Of 12 randomly selected kanamycin-resistant colonies, all were sensitive to 1 μg/mL CHIR-090. Therefore, the CHIR-090 resistance of *E. coli* W3110RL shows the expected genetic linkage to the *lpxC* locus.

The W3110RL phenotype is stable, as demonstrated by removing CHIR-090 for several generations without loss of resistance. DNA sequencing confirmed that the *R. leguminosarum lpxC* gene replaced *E. coli lpxC* without altering the native chromosomal DNA sequence upstream or downstream of the insert.

As shown by diffusion assays with 10 μg of antibiotic per disk (Figure 7), W3110 and W3110RL were equally susceptible to tobramycin and ciprofloxacin. However, W3110RL was much less sensitive to CHIR-090 than was

Table 1: Kinetics and Inhibition of *E. coli* versus *R. leguminosarum* LpxC

LpxC source	K_M (μM)	k_{cat} (s^{-1})	k_{cat}/K_M (M^{-1} s^{-1})	CHIR-090 K_i (nM)	CHIR-090 K_i* (nM)
E. coli[a]	4.0 ± 0.5	4.2 ± 1.3	11×10^5	4.0 ± 1.0[c]	0.4 ± 0.1[c] 0.5 ± 0.1[d]
E. coli[b]	2.1 ± 0.5	3.3 ± 0.2	15×10^5	nd[e]	nd
R. leguminosarum[a]	4.8 ± 0.4	1.7 ± 0.5	3.5×10^5	340 ± 60	na[f]

[a] This work. [b] Jackman et al. (*31*). [c] Determined by curve fitting. [d] Determined by linear fitting. [e] Not determined. [f] Not applicable.

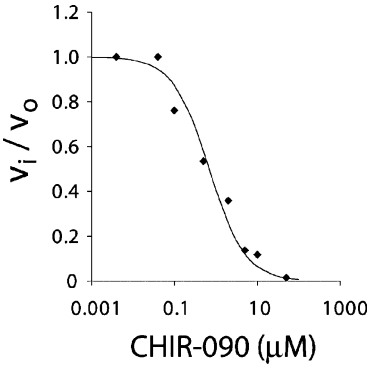

FIGURE 6: Inhibition of *R. leguminosarum* LpxC by CHIR-090. An IC_{50} for CHIR-090 inhibition of *R. leguminosarum* LpxC activity at 5 μM substrate was determined from a plot of fractional activity (v_i/v_o) versus CHIR-090 concentration. The IC_{50} value was calculated using the equation $v_i/v_o = 1/(1 + [I]/IC_{50})$, yielding an IC_{50} value of 0.69 μM. A repeat experiment (not shown) gave identical results (within 10%).

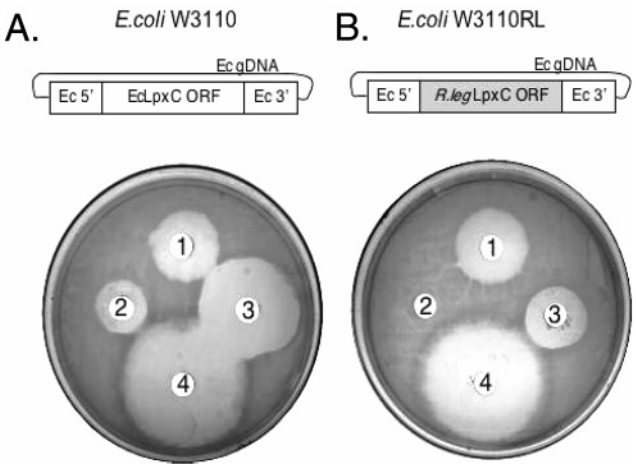

FIGURE 7: *E. coli* W3110RL is much less sensitive to CHIR-090. Disk diffusion tests were used to test for antibiotic sensitivity. Panel A: CHIR-090 inhibits the growth of the parental strain *E. coli* W3110 with potency that is intermediate between tobramycin and ciprofloxacin. Panel B: *E. coli* W3110RL is completely resistant to L-161,240 and much less sensitive to CHIR-090 than the parental strain. The compounds were tested at 10 μg per disk: tobramycin (1), L-161,240 (2), CHIR-090 (3), and ciprofloxacin (4). Abbreviations: Ec, *E. coli*; gDNA, genomic DNA; ORF, open reading frame.

W3110, and W3110RL was completely resistant to L-161,-240 (Figure 7). The MIC of CHIR-090 against W3110RL in liquid medium is 100 μg/mL, compared to 0.25 μg/mL for W3110 (data not shown). This ~400-fold reduction in sensitivity of W3110RL to CHIR-090 is consistent with the ~600-fold increase in the K_i of *R. leguminosarum* LpxC versus the K_i* of *E. coli* LpxC for CHIR-090 (Table 1).

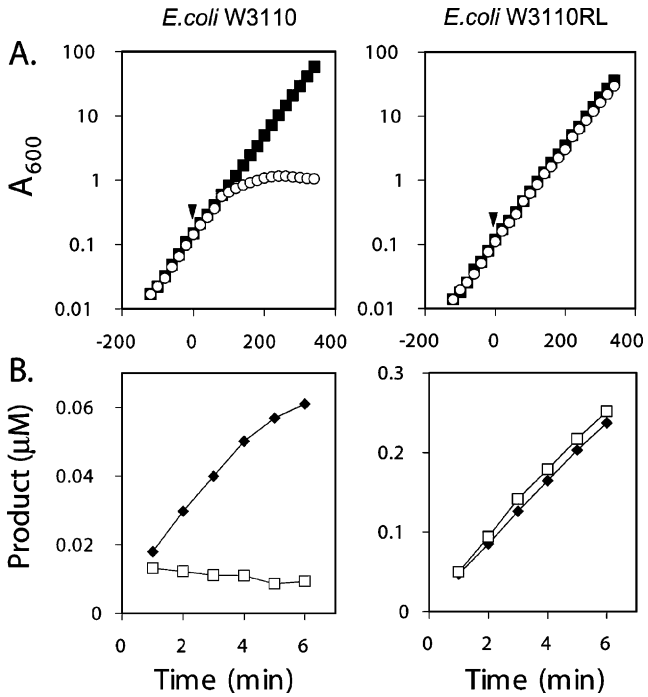

FIGURE 8: Growth of *E. coli* W3110RL in the presence of CHIR-090 and resistance of LpxC to CHIR-090 in W3110RL extracts. Panel A: The cumulative growth yield of the parental strain *E. coli* W3110 (left graph) was compared to that of *E. coli* W3110RL (right graph) when DMSO (■) or CHIR-090 dissolved in DMSO (○) was added at time 0, as indicated by the arrow. The final concentration of CHIR-090 and DMSO in the culture medium was 1 μg/mL and 0.012%, respectively. Panel B: LpxC activity in cell-free extracts of *E. coli* W3110 (left graph) or W3110RL (right graph) was measured in the presence of 10% DMSO (◆) or 10% DMSO plus 50 nM CHIR-090 (□). The concentration of the cell-free extract in the assay system was 0.83 mg/mL for *E. coli* W3110 and 0.99 mg/mL for *E. coli* W3110RL. A repeat experiment (not shown) gave identical results (within 10%).

To confirm the presence of *R. leguminosarum* LpxC activity in *E. coli* W3110RL, we assayed the cell-free extract of this strain in the presence and absence of 50 nM CHIR-090 (Figure 8B). There was no inhibition of LpxC activity in extracts of this construct, whereas LpxC activity was inhibited completely in extracts of *E. coli* W3110 (Figure 8B). *R. leguminosarum lpxC* expressed from an appropriate promoter may therefore be useful as a selectable antibiotic resistance marker in the transformation or transduction of CHIR-090-sensitive bacteria.

On the basis of these data, we conclude that LpxC is indeed the primary intracellular target for CHIR-090 in wild-type *E. coli* at concentrations up to at least 50 μg/mL.

DISCUSSION

In the present study we have demonstrated that CHIR-090 is a potent slow, tight-binding inhibitor of LpxC

orthologues from several important Gram-negative pathogens. CHIR-090 is therefore an excellent lead compound for the further development of lipid A biosynthesis inhibitors as clinical antibiotics. Because its mode of action is distinct from those of all commercial antibiotics, CHIR-090 should be effective against multidrug-resistant Gram-negative bacteria, as are often encountered in cystic fibrosis patients or debilitated individuals (*37*, *38*). As yet, the pharmacokinetics, efficacy, and safety of CHIR-090 in animal models have not been reported.

Our kinetic evaluation of *E. coli* LpxC showed that, similar to *A. aeolicus* LpxC, CHIR-090 inhibition occurs by a two-step, time-dependent mechanism with a low nanomolar K_i (1.0−1.7 nM for *A. aeolicus* LpxC versus 4.0 nM for *E. coli* LpxC) (*11*). Likewise, the *H. pylori* and *P. aeruginosa* LpxC orthologues are inhibited by low nanomolar levels of CHIR-090 in a time-dependent manner (Figure 5). A thorough analysis of inhibition kinetics is essential when evaluating therapeutic leads. Time-dependent inhibitors are highly desirable because they mitigate the effects of substrate accumulation (*37*, *38*). Slow, tight-binding effects are therefore expected to enhance the relative potency of a compound, reducing the necessary dosage and avoiding potential off-target toxic effects.

The observation that *R. leguminosarum* and related Gram-negative bacteria are resistant to CHIR-090 afforded an opportunity to validate the specificity and mechanism of this compound as an antibiotic. We found that CHIR-090 inhibits *R. leguminosarum* LpxC 600-fold less effectively than *E. coli* LpxC (Table 1). Furthermore, CHIR-090 does not display slow, tight-binding inhibition with *R. leguminosarum* LpxC, and it does not inhibit the growth of *R. leguminosarum* cells, as judged by disk diffusion assays (data not shown). The small halo of growth inhibition seen with *E. coli* W3110RL (Figure 7) in which *R. leguminosarum lpxC* replaces *E. coli lpxC* does suggest that the insensitivity of *R. leguminosarum* LpxC to CHIR-090 is not the only reason for the resistance of *R. leguminosarum* cells. This discrepancy could be explained in several ways. *E. coli* K-12 and *R. leguminosarum* (biovar *viciae* strain 3841) differ in that *R. leguminosarum* synthesizes LPS-containing O-antigen repeats, which are necessary for the establishment of symbiosis (*39*−*41*). The *R. leguminosarum* outer membrane may therefore be less permeable to CHIR-090 than that of *E. coli* W3110, which lacks O-antigen (*42*). Alternatively, CHIR-090 may be pumped out of the *R. leguminosarum* cytosol or be detoxified by a unique modification pathway. Furthermore, we cannot exclude the possibility that a secondary target for CHIR-090 accounts for the residual antibiotic activity seen with *E. coli* W3110RL (Figure 7). Given the relative resistance of W3110RL toward CHIR-090 (MIC of 100 μg/mL versus 0.25 μg/mL for W3110), we can conclude that CHIR-090 is indeed highly selective for LpxC in *E. coli* K-12 (Figure 8).

Unlike the situation with L-161,240 (*9*, *10*), spontaneous resistant colonies are not seen in disk diffusion assays with CHIR-090. Furthermore, no spontaneous resistant colonies are observed when 10^9 W3110 cells are plated onto agar containing 1 or 10 μg/mL CHIR-090. Prior to CHIR-090, the most effective LpxC inhibitor was BB-78485 (Figure 2) and the related compound BB-78484. As with L-161,240, BB-78484-resistant colonies could be isolated easily from cultures grown with BB-78484 present at 8 times its MIC (*12*). Most of the BB-78484-resistant bacteria contained single amino acid substitutions in either FabZ (*12*), the 3-hydroxyacyl-ACP dehydratase of fatty acid biosynthesis (*43*), or LpxC (*12*). Although not seen with wild-type *E. coli* W3110, CHIR-090-resistant colonies were observed in the disk diffusion assay of *E. coli* W3110RL (not visible in Figure 7B). These colonies have not yet been characterized. Taken together, the data suggest that multiple mutations in one or more genes of wild-type *E. coli* may be required to generate CHIR-090 resistance. This feature should limit the development of resistance to CHIR-090 in clinical settings.

We are currently exploring the structural basis for the insensitivity of *R. leguminosarum* LpxC to CHIR-090. Several amino acid residues that line the fatty acid binding tunnel of LpxC are not conserved in *R. leguminosarum* and related soil organisms, when compared to sensitive strains. These differences might account for the resistance of *R. leguminosarum* LpxC to CHIR-090. The NMR (*18*, *20*) and crystal (*21*, *22*) structures of the CHIR-090-sensitive *A. aeolicus* LpxC are available and should facilitate the structural analysis of *R. leguminosarum* LpxC by molecular modeling. It will also be very informative to determine a high-resolution structure of a CHIR-090-sensitive LpxC orthologue with bound CHIR-090 and to determine whether or not the biphenyl acetylene unit of CHIR-090 (Figure 2) is positioned within the fatty acid binding tunnel of LpxC. Structure-based methods were not used to design any of the available LpxC inhibitors. When the results of ongoing structural studies are incorporated into the design of new compounds, it is likely that LpxC inhibitors with greater antibiotic potency, alternative zinc binding motifs, and/or enhanced pharmacokinetics will be identified.

ACKNOWLEDGMENT

We thank Dr. Johannes Rudolph for helpful discussions, assistance with curve fitting, and a critical reading of the manuscript and Dr. Z. Guan for help with electrospray ionization mass spectrometry.

SUPPORTING INFORMATION AVAILABLE

Table S1 (primers used in this study) and Table S2 (purification of LpxC orthologues). This material is available free of charge via the Internet at http://pubs.acs.org.

REFERENCES

1. Levy, S. B. (2005) Antibiotic resistance-the problem intensifies, *Adv. Drug Deliv. Rev. 57*, 1446−1450.
2. Levy, S. B., and Marshall, B. (2004) Antibacterial resistance worldwide: causes, challenges and responses, *Nat. Med. 10*, S122−S129.
3. Wright, M. O. (2005) Multi-resistant gram-negative organisms in Maryland: a statewide survey of resistant *Acinetobacter baumannii*, *Am. J. Infect. Control 33*, 419−421.
4. Walsh, C. T. (2003) Where will new antibiotics come from?, *Nat. Rev. Microbiol. 1*, 65−70.
5. Projan, S. J. (2002) New (and not so new) antibacterial targets—from where and when will the novel drugs come?, *Curr. Opin. Pharmacol. 2*, 513−522.
6. Gerdes, S. Y., Scholle, M. D., Campbell, J. W., Balazsi, G., Ravasz, E., Daugherty, M. D., Somera, A. L., Kyrpides, N. C., Anderson, I., Gelfand, M. S., Bhattacharya, A., Kapatral, V., D'Souza, M., Baev, M. V., Grechkin, Y., Mseeh, F., Fonstein, M. Y., Overbeek, R., Barabasi, A. L., Oltvai, Z. N., and Osterman,

A. L. (2003) Experimental determination and system level analysis of essential genes in *Escherichia coli* MG1655, *J. Bacteriol. 185*, 5673−5684.
7. Raetz, C. R. H. (1990) Biochemistry of endotoxins, *Annu. Rev. Biochem. 59*, 129−170.
8. Raetz, C. R. H., and Whitfield, C. (2002) Lipopolysaccharide endotoxins, *Annu. Rev. Biochem. 71*, 635−700.
9. Onishi, H. R., Pelak, B. A., Gerckens, L. S., Silver, L. L., Kahan, F. M., Chen, M. H., Patchett, A. A., Galloway, S. M., Hyland, S. A., Anderson, M. S., and Raetz, C. R. H. (1996) Antibacterial agents that inhibit lipid A biosynthesis, *Science 274*, 980−982.
10. Jackman, J. E., Fierke, C. A., Tumey, L. N., Pirrung, M., Uchiyama, T., Tahir, S. H., Hindsgaul, O., and Raetz, C. R. H. (2000) Antibacterial agents that target lipid A biosynthesis in gram-negative bacteria. Inhibition of diverse UDP-3-*O*-(*R*-3-hydroxymyristoyl)-*N*-acetylglucosamine deacetylases by substrate analogs containing zinc binding motifs, *J. Biol. Chem. 275*, 11002−11009.
11. McClerren, A. L., Endsley, S., Bowman, J. L., Andersen, N. H., Guan, Z., Rudolph, J., and Raetz, C. R. H. (2005) A slow, tight-binding inhibitor of the zinc-dependent deacetylase LpxC of lipid A biosynthesis with antibiotic activity comparable to ciprofloxacin, *Biochemistry 44*, 16574−16583.
12. Clements, J. M., Coignard, F., Johnson, I., Chandler, S., Palan, S., Waller, A., Wijkmans, J., and Hunter, M. G. (2002) Antibacterial activities and characterization of novel inhibitors of LpxC, *Antimicrob. Agents Chemother. 46*, 1793−1799.
13. Anderson, M. S., Bulawa, C. E., and Raetz, C. R. H. (1985) The biosynthesis of gram-negative endotoxin: formation of lipid A precursors from UDP-GlcNAc in extracts of *Escherichia coli*, *J. Biol. Chem. 260*, 15536−15541.
14. Anderson, M. S., Robertson, A. D., Macher, I., and Raetz, C. R. H. (1988) Biosynthesis of lipid A in *Escherichia coli*: identification of UDP-3-*O*-(*R*-3-hydroxymyristoyl)-α-D-glucosamine as a precursor of UDP-N^2-O^3-*bis*-(*R*-3-hydroxymyristoyl)-α-D-glucosamine, *Biochemistry 27*, 1908−1917.
15. Anderson, M. S., Bull, H. S., Galloway, S. M., Kelly, T. M., Mohan, S., Radika, K., and Raetz, C. R. H. (1993) UDP-*N*-acetylglucosamine acyltransferase of *Escherichia coli*: the first step of endotoxin biosynthesis is thermodynamically unfavorable, *J. Biol. Chem. 268*, 19858−19865.
16. Sorensen, P. G., Lutkenhaus, J., Young, K., Eveland, S. S., Anderson, M. S., and Raetz, C. R. H. (1996) Regulation of UDP-3-*O*-[*R*-3-hydroxymyristoyl]-*N*-acetylglucosamine deacetylase in *Escherichia coli*. The second enzymatic step of lipid A biosynthesis, *J. Biol. Chem. 271*, 25898−25905.
17. McClerren, A. L., Zhou, P., Guan, Z., Raetz, C. R. H., and Rudolph, J. (2005) Kinetic analysis of the zinc-dependent deacetylase in the lipid A biosynthetic pathway, *Biochemistry 44*, 1106−1113.
18. Coggins, B. E., McClerren, A. L., Jiang, L., Li, X., Rudolph, J., Hindsgaul, O., Raetz, C. R. H., and Zhou, P. (2005) Refined solution structure of the LpxC-TU-514 complex and pK_a analysis of an active site histidine: insights into the mechanism and inhibitor design, *Biochemistry 44*, 1114−11126.
19. Hernick, M., Gennadios, H. A., Whittington, D. A., Rusche, K. M., Christianson, D. W., and Fierke, C. A. (2005) UDP-3-*O*-((*R*)-3-hydroxymyristoyl)-*N*-acetylglucosamine deacetylase functions through a general acid-base catalyst pair mechanism, *J. Biol. Chem. 280*, 16969−16978.
20. Coggins, B. E., Li, X., McClerren, A. L., Hindsgaul, O., Raetz, C. R. H., and Zhou, P. (2003) Structure of the LpxC deacetylase with a bound substrate-analog inhibitor, *Nat. Struct. Biol. 10*, 645−651.
21. Whittington, D. A., Rusche, K. M., Shin, H., Fierke, C. A., and Christianson, D. W. (2003) Crystal structure of LpxC, a zinc-dependent deacetylase essential for endotoxin biosynthesis, *Proc. Natl. Acad. Sci. U.S.A. 100*, 8146−8150.
22. Gennadios, H. A., Whittington, D. A., Li, X., Fierke, C. A., and Christianson, D. W. (2006) Mechanistic inferences from the binding of ligands to LpxC, a metal-dependent deacetylase, *Biochemistry 45*, 7940−7948.
23. Kline, T., Andersen, N. H., Harwood, E. A., Bowman, J., Malanda, A., Endsley, S., Erwin, A. L., Doyle, M., Fong, S., Harris, A. L., Mendelsohn, B., Mdluli, K., Raetz, C. R. H., Stover, C. K., Witte, P. R., Yabannavar, A., and Zhu, S. (2002) Potent, novel in vitro inhibitors of the *Pseudomonas aeruginosa* deacetylase LpxC, *J. Med. Chem. 45*, 3112−3129.
24. Pirrung, M. C., Tumey, L. N., McClerren, A. L., and Raetz, C. R. H. (2003) High-throughput catch-and-release synthesis of oxazoline hydroxamates. Structure-activity relationships in novel inhibitors of *Escherichia coli* LpxC: in vitro enzyme inhibition and antibacterial properties, *J. Am. Chem. Soc. 125*, 1575−1586.
25. Mdluli, K. E., Witte, P. R., Kline, T., Barb, A. W., Erwin, A. L., Mansfield, B. E., McClerren, A. L., Pirrung, M. C., Tumey, L. N., Warrener, P., Raetz, C. R. H., and Stover, C. K. (2006) Molecular validation of LpxC as an antibacterial drug target in *Pseudomonas aeruginosa*, *Antimicrob. Agents Chemother. 50*, 2178−2184.
26. Kanjilal-Kolar, S., Basu, S. S., Kanipes, M. I., Guan, Z., Garrett, T. A., and Raetz, C. R. H. (2006) Expression cloning of three *Rhizobium leguminosarum* lipopolysaccharide core galacturonosyltransferases, *J. Biol. Chem. 281*, 12865−12878.
27. Hyland, S. A., Eveland, S. S., and Anderson, M. S. (1997) Cloning, expression, and purification of UDP-3-*O*-acyl-GlcNAc deacetylase from *Pseudomonas aeruginosa*: a metalloamidase of the lipid A biosynthesis pathway, *J. Bacteriol. 179*, 2029−2037.
28. Andersen, N. H., Bowman, J., Erwin, A., Harwood, E., Kline, T., Mdluli, K., Pfister, K. B., Shawar, R., Wagman, A., and Yabannavar, A. (2004) Antibacterial Agents, *World Intellectual Property Organization*, Patent WO 2004/062601 A2, pp 324, Chiron, Emeryville, CA.
29. Miller, J. R. (1972) *Experiments in Molecular Genetics*, Cold Spring Harbor Laboratory, Cold Spring Harbor, NY.
30. Smith, P. K., Krohn, R. I., Hermanson, G. T., Mallia, A. K., Gartner, F. H., Provenzano, M. D., Fujimoto, E. K., Goeke, N. M., Olson, B. J., and Klenk, D. C. (1985) Measurement of protein using bicinchoninic acid, *Anal. Biochem. 150*, 76−85.
31. Jackman, J. E., Raetz, C. R. H., and Fierke, C. A. (1999) UDP-3-*O*-(*R*-3-hydroxymyristoyl)-*N*-acetylglucosamine deacetylase of *Escherichia coli* is a zinc metalloenzyme, *Biochemistry 38*, 1902−1911.
32. Copeland, R. A. (2005) *Evaluation of enzyme inhibitors in drug discovery: a guide for medicinal chemists and pharmacologists*, Wiley-Interscience, Hoboken, NJ.
33. Morrison, J. F., and Walsh, C. T. (1988) The behavior and significance of slow-binding enzyme inhibitors, *Adv. Enzymol. Relat. Areas Mol. Biol. 61*, 201−301.
34. Dowd, J. E., and Riggs, D. S. (1965) A comparison of estimates of Michaelis-Menten kinetic constants from various linear transformations, *J. Biol. Chem. 240*, 863−869.
35. Datsenko, K. A., and Wanner, B. L. (2000) One-step inactivation of chromosomal genes in *Escherichia coli* K-12 using PCR products, *Proc. Natl. Acad. Sci. U.S.A. 97*, 6640−6645.
36. Stacey, G., Burris, R. H., and Evans, H. J. (1992) *Biological Nitrogen Fixation*, p 943, Routledge, Chapman, and Hall, New York.
37. Conway, S. P., Brownlee, K. G., Denton, M., and Peckham, D. G. (2003) Antibiotic treatment of multidrug-resistant organisms in cystic fibrosis, *Am. J. Respir. Med. 2*, 321−332.
38. Garau, J., and Gomez, L. (2003) *Pseudomonas aeruginosa* pneumonia, *Curr. Opin. Infect. Dis. 16*, 135−143.
39. de Maagd, R. A., Rao, A. S., Mulders, I. H., Goosen-de, Roo, L., van Loosdrecht, M. C., Wijffelman, C. A., and Lugtenberg, B. J. (1989) Isolation and characterization of mutants of *Rhizobium leguminosarum* bv. viciae 248 with altered lipopolysaccharides: possible role of surface charge or hydrophobicity in bacterial release from the infection thread, *J. Bacteriol. 171*, 1143−1150.
40. Carlson, R. W., Reuhs, B., Chen, T. B., Bhat, U. R., and Noel, K. D. (1995) Lipopolysaccharide core structures in *Rhizobium etli* and mutants deficient in O-antigen, *J. Biol. Chem. 270*, 11783−11788.
41. Noel, K. D., Forsberg, L. S., and Carlson, R. W. (2000) Varying the abundance of O antigen in *Rhizobium etli* and its effect on symbiosis with *Phaseolus vulgaris*, *J. Bacteriol. 182*, 5317−5324.
42. Stevenson, G., Neal, B., Liu, D., Hobbs, M., Packer, N. H., Batley, M., Redmond, J. W., Lindquist, L., and Reeves, P. (1994) Structure of the O-antigen of *Escherichia coli* K-12 and the sequence of its *rfb* gene cluster, *J. Bacteriol. 176*, 4144−4156.
43. Mohan, S., Kelly, T. M., Eveland, S. S., Raetz, C. R. H., and Anderson, M. S. (1994) An *Escherichia coli* gene (*fabZ*) encoding *R*-3-hydroxymyristoyl acyl carrier protein dehydrase. Relation to *fabA* and suppression of mutations in lipid A biosynthesis, *J. Biol. Chem. 269*, 32896−32903.
44. Raetz, C. R. H., Garrett, T. A., Reynolds, C. M., Shaw, W. A., Moore, J. D., Smith, D. C., Jr., Ribeiro, A. A., Murphy, R. C.,

Ulevitch, R. J., Fearns, C., Reichart, D., Glass, C. K., Benner, C., Subramaniam, S., Harkewicz, R., Bowers-Gentry, R. C., Buczynski, M. W., Cooper, J. A., Deems, R. A., and Dennis, E. A. (2006) Kdo2-Lipid A of *Escherichia coli*, a defined endotoxin that activates macrophages via TLR-4, *J. Lipid Res. 47*, 1097−1111.

BI6025165